

Corrosion of the crystalline phases of matte glazes in aqueous solutions

Linda Fröberg*, Leena Hupa, Mikko Hupa

Process Chemistry Centre, Åbo Akademi University, Biskopsgatan 8, FI-20500 Turku, Finland

Received 25 June 2007; received in revised form 14 February 2008; accepted 18 April 2008

Available online 7 September 2008

Abstract

Chemical durability was determined for fast and conventionally fired matte raw glazes in acidic to alkaline aqueous solutions. According to XRD, the main crystalline phases in the glazes were diopside, plagioclase, anorthite, wollastonite, and pseudowollastonite. SEM-EDXA and whitelight confocal microscopy were used to analyze the surfaces after immersion in the aqueous solutions. The ionic concentrations in selected solutions after immersion were determined by ICP-AES. Diopside was not attacked by the test solutions. Plagioclase started to corrode along the crystal interfaces in the most acidic environments. Wollastonite crystals with different crystal habitus and slightly different chemical composition formed depending on firing cycle and composition of the glaze. In fast firing, tiny columnar wollastonite crystals were formed. These crystals were attacked in acidic to slightly alkaline environments. In conventionally fired glazes the wollastonite crystals were dendritic. These crystals were attacked only by acidic solutions. Pseudowollastonite with poor chemical resistance formed only in magnesia-free glazes.

© 2008 Elsevier Ltd. All rights reserved.

Keywords: Chemical properties; Corrosion; Glass–ceramics; Glaze

1. Introduction

Chemical durability of glazes in aqueous solutions is good except in highly acidic or alkaline environments. The high alumina and silica, as well as low alkali oxide contents of the glazes make them superior to conventional soda-lime type glasses. pH of the attacking medium and the length and temperature of the exposure are the major factors inducing aqueous corrosion of ceramic coatings.¹

Chemical durability of glazes is often discussed in terms of the durability of the glassy phase. In acidic solutions hydrogen ions are assumed to replace alkali ions in the glass network, while in alkaline solutions the silica network is attacked. However, matte glazes also contain crystals embedded in the glassy phase. The crystal type varies with the glaze composition, but anorthite ($\text{CaO}\cdot\text{Al}_2\text{O}_3\cdot 2\text{SiO}_2$), mullite ($3\text{Al}_2\text{O}_3\cdot 2\text{SiO}_2$) and wollastonite ($\text{CaO}\cdot\text{SiO}_2$) are frequently observed.² Few studies have been published on the chemical resistance of matte glazes in aqueous solutions. Diopside and anorthite in glass–ceramics have been found to be of excellent durability in alkaline to acidic solutions.^{3–5} Recently, wollastonite-type crystals in matte glazes

were reported to be readily attacked by acidic to slightly alkaline solutions.^{6–11} The mechanisms of the wollastonite corrosion were not fully understood, but the corrosion was suggested mainly along the interfacial layer between the crystals and glassy phase.

In industry chemical durability of glazed surfaces is often classified by visual method according to the ISO 10545-13 standard. The visual method is well suited for product control and overall estimation and comparison of the surface quality, color, and gloss. It is not sufficient, however, for estimating long-term chemical durability or micro-level reactions of the surface. Understanding the reactions occurring on micro-level is important in developing glaze compositions. A damaged microstructure leads to pitting of the surface and thus to increased soiling and diminished cleanability.⁸ More accurate methods than simple visual inspection are required to classify the behavior of surfaces in aqueous environments. Recently, corrosion of glazes has been studied by whitelight confocal microscopy, scanning electron microscopy, and atomic force microscopy.^{6–8,12–14}

The purpose of this work was to shade light on corrosion mechanisms of glazed surfaces in order to develop more durable surfaces. The elemental compositions of the different crystalline phases observed in matte glazes were investigated in detail. The focus was on understanding the corrosion mechanisms of

* Corresponding author. Tel.: +358 2 215 4421; fax: +358 2 215 4962.
E-mail address: linda.froberg@abo.fi (L. Fröberg).

Table 1
Oxide compositions (wt%) and main crystal types in the surfaces of the experimental glazes after fast or conventional firing according to XRD

Glaze	Na ₂ O	K ₂ O	MgO	CaO	Al ₂ O ₃	SiO ₂	Main crystal (XRD)	
							Fast firing	Conventional
2	1.8 ± 0.2	2.2 ± 0.2	4.0 ± 0.1	17.5 ± 0.3	25.0 ± 0.3	49.5 ± 0.4	D	An
3	1.8 ± 0.2	2.3 ± 0.2	4.0 ± 0.1	17.4 ± 0.3	10.1 ± 0.1	54.5 ± 0.7	D, W	D
4	2.8 ± 0.3	3.4 ± 0.3	3.8 ± 0.1	16.8 ± 0.2	11.7 ± 0.1	61.4 ± 0.8	D, W	D
5	1.8 ± 0.2	2.3 ± 0.2	0.1 ± 0.1	17.4 ± 0.4	10.0 ± 0.1	68.4 ± 0.8	PW	PW
9	3.0 ± 0.3	3.6 ± 0.3	0.2 ± 0.2	28.9 ± 0.3	12.3 ± 0.1	52.1 ± 0.9	PW	PW
11	3.2 ± 0.3	3.8 ± 0.3	2.0 ± 0.1	17.5 ± 0.3	17.5 ± 0.2	56.0 ± 0.8	W	W
13	3.2 ± 0.3	3.8 ± 0.3	0.2 ± 0.2	30.0 ± 0.3	17.7 ± 0.3	45.4 ± 0.8	PW	PW
14	4.5 ± 0.4	5.2 ± 0.4	3.6 ± 0.1	5.8 ± 0.	24.5 ± 0.3	56.4 ± 0.7	D	Pc

Pc, plagioclase; An, anorthite; D, diopside; W, wollastonite; PW, pseudowollastonite.

wollastonite and pseudowollastonite, i.e. the two crystalline phases that are easily attacked in aqueous solutions. Corrosion was established by (i) analyzing the glazed surfaces before and after immersion using different microscopic techniques, and (ii) analyzing the immersion solutions by ICP-AES.

2. Materials and methods

Chemical durability of eight glazes given in Table 1 was studied in acidic to alkaline solutions (Table 1). The nominal compositions as well as the standard deviations were based on variations in composition of the commercial raw materials (feldspar, quartz, corundum, kaolin, limestone, and dolomite) used for the batches. The glazes were selected from an experimental series of fifteen raw glazes within the composition range for commercial floor tiles and sanitary ware fired at peak temperature 1215 °C according to a fast-firing cycle in an industrial kiln and a conventional firing schedule in a laboratory furnace (Carbolite RHF 16/35).^{13,15} All glazes in this corrosion study had a high ratio of crystalline to amorphous phase ratio.

2.1. Characterizing the experimental surfaces

Phase composition of the glazes was analyzed by X-ray diffraction (X'pert by Philips, Cu α radiation, 2θ from 5° to 65° with a step size of 0.02° and a step time 5 s). A scanning electron microscope equipped for energy dispersive X-ray analysis (FEG-SEM, LEO 1530 from Zeiss/EDXA from Vantage by Thermo Electron Corporation) was used for surface analysis of the glazes both before and after the immersion tests. Surface topography and average surface roughness (Sa) were measured by spinning disk whitelight confocal microscopy (COM, NanoFocus μsurf[®]) before and after immersion.

2.2. Corrosion tests

The corrosion tests were performed according to the arrangement suggested by the ISO 10545-13 standard. A glass tube, fastened with modeling clay to the glaze surface was filled with 17 ml of test solution. After the specified testing time, from 5 min, to 4 days, the solution was removed and the surface was analyzed by SEM-EDX and COM. Because the contamination risk from the modeling clay was high, analysis of the immer-

sion solutions were done with an experimental arrangement in which a Teflon ring (inner diameter 28 mm, height 20.5 mm) with a silicon O-ring was tightly fastened to the glaze surface with spring clips. The total volume of the test solution was now 10 ml. The smaller volume gave higher concentrations of ions dissolved from the glaze and thus enabled the detection of changes in the solution also due to minor dissolution of the surface.

Chemical durability was tested by immersing the glazes for different periods of time, in ultra pure water (pH 5.7), citric acid (pH 1.5), hydrochloric acid (pH 2.9), weakly alkaline detergent (pH 9.1), and potassium hydroxide (pH 13.4) solutions. After immersion, changes in surface morphology as a result of corrosion were analyzed by SEM-EDXA and COM. Ion concentrations in the hydrochloric acid solution after immersion were determined by inductive coupled plasma-atom emission spectrometry (ICP-AES, Thermo Jarrell Ash AtomScanTM 25 with the program ThermoSPEC version 6.20). Six parallel tests were performed for each sample. One wollastonite and one pseudowollastonite glaze (conventionally fired glaze 11 and fast-fired glaze 13) were selected for more detailed study on the corrosion mechanisms. For these glazes, *in situ* pH was measured in hydrochloric acid and ultra pure water.

3. Results and discussion

3.1. Phase composition

Diopside, wollastonite or pseudowollastonite together with some residual quartz and corundum were identified by X-ray analysis in the fast-fired glazes.^{14,15} In the conventionally fired glazes the initially formed crystals either grew in size or contributed to the formation of anorthite or plagioclase-type crystals.¹⁵ Two fast-fired glazes (glazes 4 and 13) and six conventionally fired glazes (glazes 2, 3, 5, 9, 11, and 14) were chosen for the corrosion tests in this work. Typical diffractograms for diopside (glaze 3), wollastonite (glaze 11), pseudowollastonite (glaze 13), anorthite (glaze 2) and plagioclase (glaze 14) are shown in Fig. 1. The main crystal types in each glaze according to X-ray analysis are given in Table 1.

Fig. 2 shows backscattered SEM-micrographs of the glazes given in Fig. 1. The average composition and the shape of the

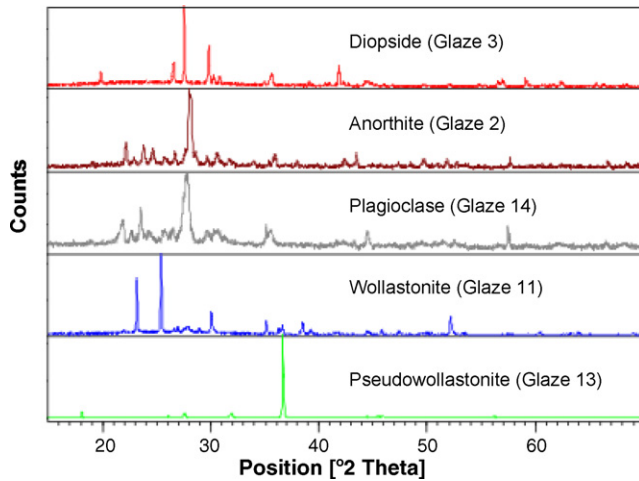


Fig. 1. X-ray diffractograms of diopside (glaze 3, conventionally fired), anorthite (glaze 2, conventionally fired), plagioclase (glaze 14, conventionally fired), wollastonite (glaze 11, conventionally fired) and pseudowollastonite (glaze 13, fast-fired) in the experimental surfaces.

crystals according to SEM-EDX analysis are given in Table 2. The compositions are based on 4–8 analyses on crystals on each surface. In the quantitative EDX analysis ZAF correction procedures with default standards were applied and calculated into oxides. Although the laser-beam width in the analysis was adjusted to give only the composition of the crystalline phases, also the glassy phase surrounding the crystals was likely to partly interfere with the data.

3.1.1. Plagioclase

Alkaline oxides were found only in the crystals of the glazes which according to XRD contained either plagioclase or anorthite (Table 2). The lime rich crystals in the plagioclase system were referred to as anorthite, while all other solid solutions in the albite-anorthite system were referred to as plagioclase. Columnar crystals with a composition suggesting plagioclase (by XRD analysis) were observed only in glazes with very low silica content and relatively high feldspar and corundum contents. The SEM-micrographs of plagioclase showed a network of columnar crystals with interlocking grain boundaries (Fig. 2). The feldspar used for manufacturing the glazes consisted of roughly equal amounts of orthoclase and albite. The

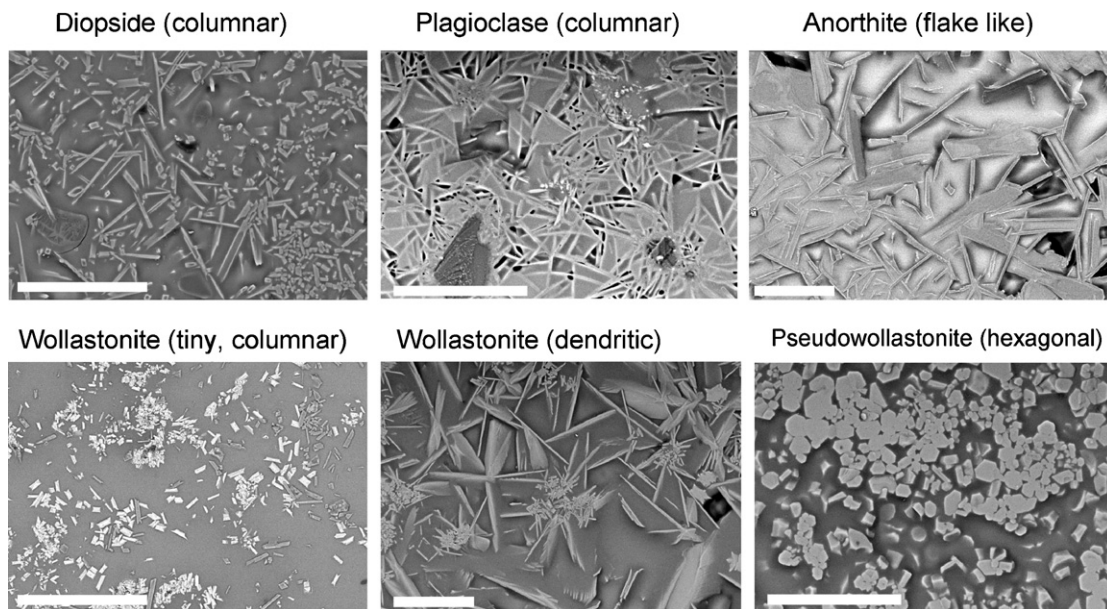


Fig. 2. Backscattered SEM-micrographs showing the typical shapes of crystals in the glazes given in Table 1. Columnar diopside (glaze 3), columnar plagioclase (glaze 14), flake-like anorthite (glaze 2), columnar wollastonite (glaze 4), dendritic wollastonite (glaze 11), and hexagonal pseudowollastonite (glaze 13). The bars equals to 40 μm .

Table 2
Shape and an average oxide composition of the crystals according SEM-EDXA

Crystal	Crystal shape (SEM)	Composition (mol%) of crystal (EDXA)					
		Na ₂ O	K ₂ O	Al ₂ O ₃	MgO	CaO	SiO ₂
Diopside	Columnar	0	0	1	23.5	24	51.5
Plagioclase	Columnar	14	9	37	6	20	14
Anorthite	Flake	2	1	16	3	17	61
Wollastonite	Columnar	0	0	1	2.5	42	55.5
Wollastonite	Dendritic	0	0	2	2	43	53
Pseudowollastonite	Hexagonal	0	0	1	0	47	52

Table 3
Corrosion of different crystals in aqueous solutions of different pH

Solution	pH	Immersion time at which corrosion observed					
		D	Pc (day)	An	W1	W2	PW
Citric acid	1.5	–	1	–	Minutes	1 h	Minutes
HCl	2.9	–	1–4	–	1 h	4 h	Minutes
Water	5.7	–	–	–	2 d	–	1 d
Detergent	9.1	–	–	–	1–4 d	–	1–10 h
KOH	13.4	–, ✖	–, ✖	–	–, ✖	–, ✖	–, ✖

D, diopside; Pc, plagioclase; An, anorthite; W1, columnar wollastonite; W2, dendritic wollastonite; PW, pseudowollastonite; (–) no corrosion; (✖), corrosion of glassy phase within 1 day.

composition of the plagioclase crystals suggested that they were formed by reactions between corundum and feldspar. Alternatively, dissolution of alumina in the feldspar-rich melt led to precipitation of plagioclase. As the crystals were needle-like with a high aspect ratio, the composition given by EDX analysis had likely interfered with the surrounding glassy phase and some residual corundum. This might partly explain why the average composition of the plagioclase crystals was found to be rather low in silica and high in alumina compared to typical plagioclases.

3.1.2. Anorthite

Flake-like anorthite formed in glazes with low to moderate feldspar and relatively high lime contents. Thus, anorthite was assumed to form through a reaction between lime, alumina and quartz.

3.1.3. Diopside

In glazes with the molar ratio of magnesia to lime >0.2 diopside crystals were observed.¹⁵ The crystals were columnar in both firings. The crystal length was 2–5 μm in fast firing and 2–40 μm in conventional firing. If the ratio was around 0.2, wollastonite and diopside were observed in the same glaze. Under prolonged firing, however, the wollastonite crystals either grew in size or dissolved in the glassy phase depending on the total glaze composition. In glazes 3 and 4, where both wollastonite and diopside were formed in fast firing, the wollastonite crystals dissolved under prolonged firing leaving diopside as the main crystal phase.

3.1.4. Wollastonite

Wollastonite was observed as the major crystalline phase in fast-fired glazes with molar ratio of magnesia to lime <0.2. The crystals were tiny (2–5 μm) and columnar. According to SEM-EDX analysis, the chemical composition of the columnar crystals was roughly the same whatever the total glaze composition. With prolonged firing time the crystals grew in size and the crystal habit changed into long (5–45 μm) dendrites. SEM-EDX analysis suggested slight differences mainly in the alumina content of the dendritic and the columnar wollastonite crystals (Table 2). It was assumed that at the longer maturing time more aluminum was dissolved as solid solution within the wollastonite crystals.

3.1.5. Pseudowollastonite

Hexagonal pseudowollastonite crystals (\varnothing 2–10 μm) were found only in glazes where the molar ratio of magnesia to lime was less than 0.01. The oxide composition of the crystals was not affected by the firing time. According to EDX analysis also these crystals contained some alumina, but less than the dendritic wollastonite crystals (Table 2).

3.2. Chemical resistance

Observations on the overall corrosion tendency of the crystalline phases in the experimental glazes in the acidic to alkaline aqueous solutions as suggested by SEM micrographs of the surfaces are summarized in Table 3. Average concentrations of the

Table 4
Average concentrations of ions (mmol/dm³) dissolved from glazes containing different crystals during immersion in HCl by ICP-AES analysis

Main crystal type	Immersion time (days)	Average concentration (mmol/dm ³)					
		K ⁺	Na ⁺	Mg ²⁺	Al ³⁺	Ca ²⁺	Si ⁴⁺
Diopside	1	–	–	–	0.006	0.004	0.005
	4	–	–	0.001	–	0.006	0.015
Anorthite	1	–	–	0.001	–	0.006	0.007
	4	–	–	0.001	–	0.012	0.012
Plagioclase	1	–	0.008	0.077	0.021	0.033	0.098
	4	–	0.010	0.072	0.022	0.030	0.094
Wollastonite (dendritic)	1	–	0.003	0.009	0.010	0.154	0.051
Pseudowollastonite	1	0.039	0.049	0.002	0.037	0.963	0.335

(–) Below detection limit.

ions dissolved from the surfaces in the hydrochloric acid solution given by ICP-AES analysis are shown in Table 4.

3.2.1. Corrosion of diopside

Chemical resistance of surfaces with diopside was good in all test solutions (Table 3). SEM and COM images recorded after immersion showed no signs of attack on diopside. ICP-AES analysis of the hydrochloric solution from the test with the conventionally fired diopside glaze showed slightly increased silicon and calcium ion concentrations after 1 and 4 days of immersion (Table 4). However, the levels were under the limit for reliable detection and therefore not taken as an indication on the dissolution of diopside. Likewise, the level of magnesia in the solution was below the level of reliable detection, which further suggested that diopside had not corroded.

3.2.2. Corrosion of plagioclase

SEM-micrographs indicated weak signs of corrosion of columnar plagioclase mainly in the interfacial layer between the crystal and the glassy phase after immersion in citric and hydrochloric acids. Also some signs of corrosion were observed on the crystals, cf. SEM-micrograph in Fig. 3. The crystals

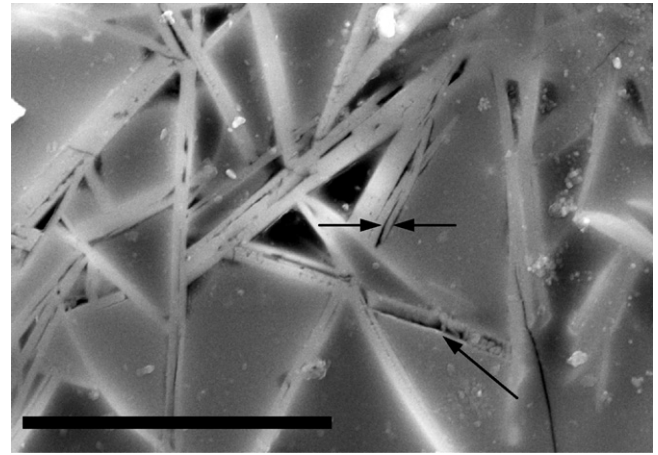


Fig. 3. SEM-micrograph showing corrosion (black arrows) mainly along interfacial layers of plagioclase (glaze 14) after 4 days in hydrochloric acid. The bar equals to 10 μm .

were not attacked by water, weakly alkaline detergent, or potassium hydroxide solutions. ICP-AES analysis showed slightly increased levels of silicon, calcium, aluminum, magnesium, and sodium ions in the hydrochloric acid solution after immersion,

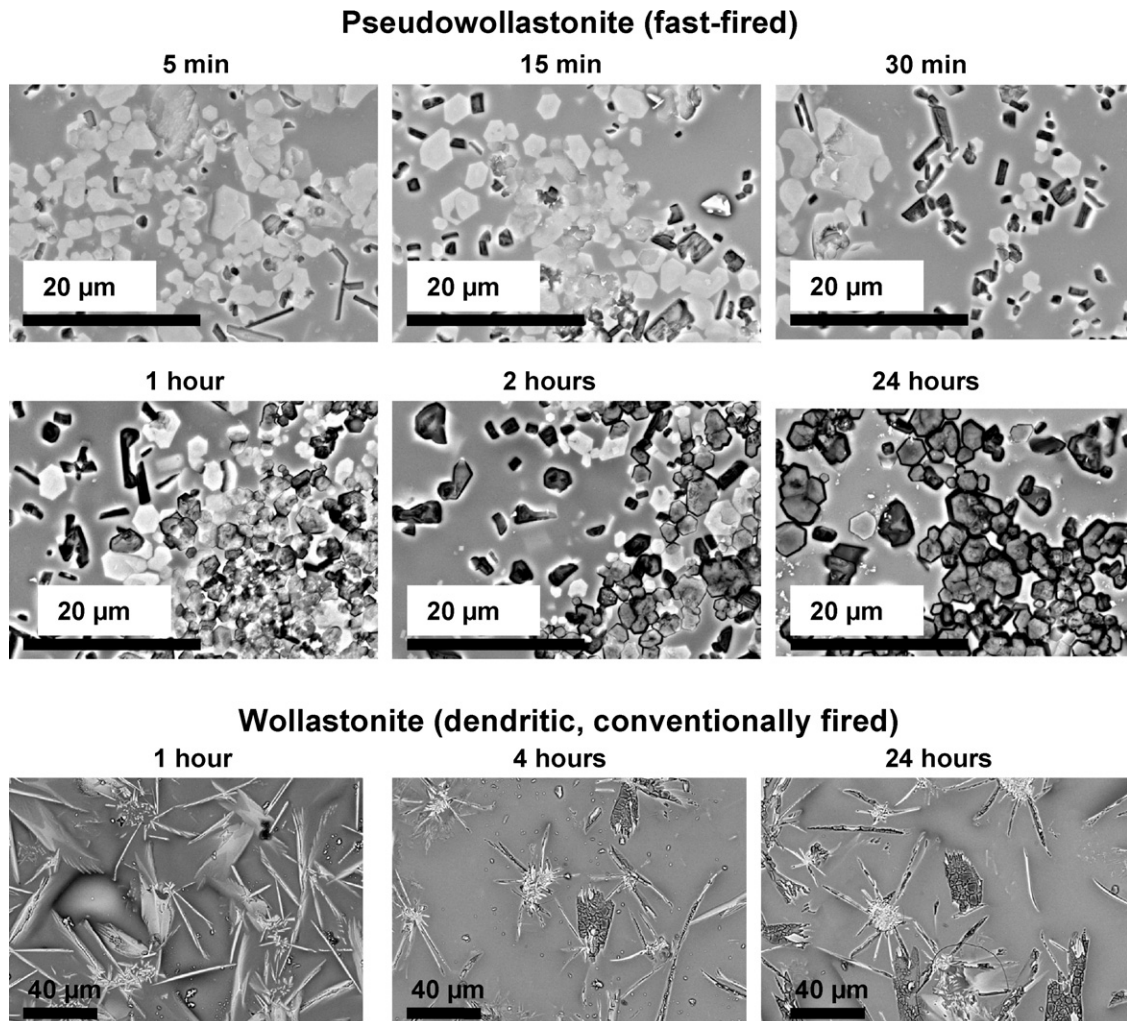


Fig. 4. SEM-micrographs of corrosion of pseudowollastonite (glaze 13) and dendritic wollastonite (glaze 11) after immersion in hydrochloric acid.

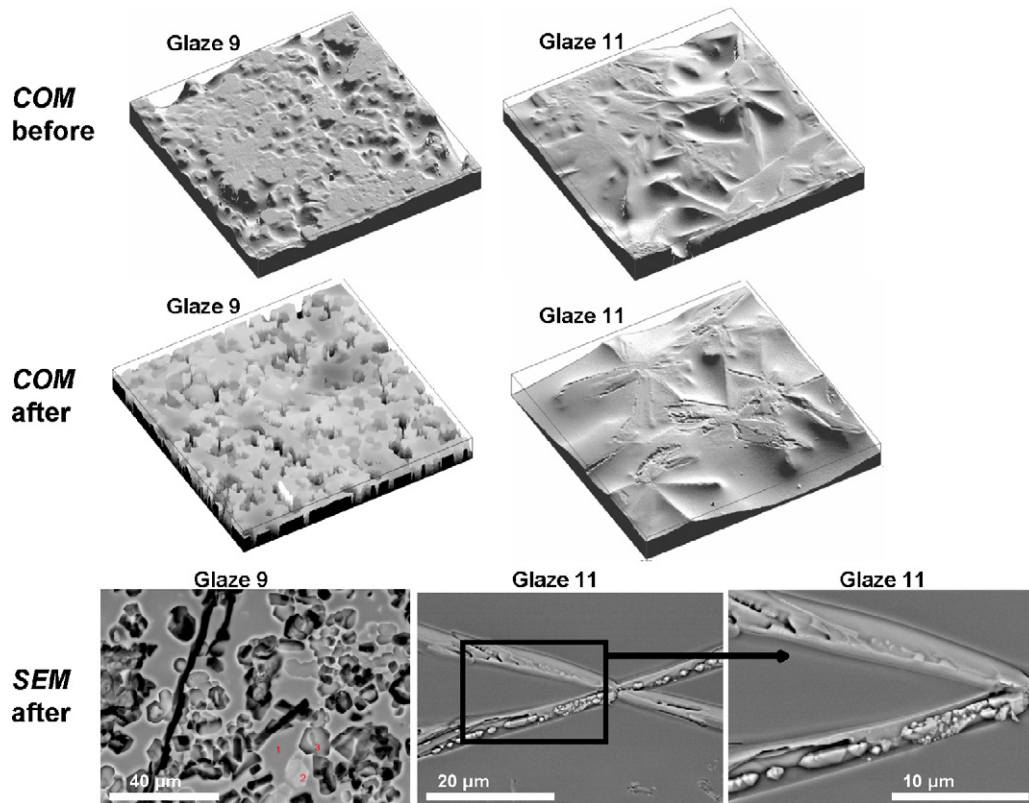


Fig. 5. Corrosion of pseudowollastonite crystals (glaze 9) and dendritic wollastonite crystals (glaze 11) after 1 h in citric acid by COM and SEM-micrographs. Image size COM: $160\ \mu\text{m} \times 158\ \mu\text{m}$.

cf. Table 4. Also the ion composition of the solutions suggested that both the glassy phase and crystals had partially corroded.

3.2.3. Corrosion of anorthite

No signs of attack on the flake-like anorthite in any of the test solutions could be observed by SEM. Only minor changes were observed in the ion concentrations of the hydrochloric acid solution. It was assumed that as anorthite formed in glazes with high corundum contents, also the glassy phase was high in alumina, thus leading to increased durability of the surface.

3.2.4. Corrosion of wollastonite and pseudowollastonite

Corrosion of the wollastonite and pseudowollastonite crystal was studied with several methods. The slight differences in the chemical composition of the crystals seemed to affect their chemical resistance. The tiny columnar wollastonite and the pseudowollastonite crystals were easily dissolved all but the most alkaline solution (Table 3). The dendritic wollastonite better withstood the neutral to alkaline environments; it was not dissolved by water or the solutions of potassium hydroxide or the weakly alkaline detergent.

First signs of attack on pseudowollastonite and tiny columnar wollastonite could be seen in the SEM-micrographs already after 5 min, in citric or hydrochloric acid. The influence of the immersion time in hydrochloric acid on the corrosion of pseudowollastonite (glaze 13) and dendritic wollastonite (glaze 11) is shown by the SEM-micrographs in Fig. 4. A clear attack on the dendritic wollastonite was not detected before 1 h, immersion.

On large crystals early signs of attack could be detected also in the COM topography images. Fig. 5 shows COM and SEM-micrographs of pseudowollastonite (glaze 9) and dendritic wollastonite (glaze 11) after 1 h, in citric acid. Severe corrosion due to leaching of pseudowollastonite was indicated by the large holes in COM images and black areas in the SEM-micrographs. Partly dissolution of dendritic wollastonite crystals was given by the pits on crystal surfaces in both COM and SEM-micrographs.

Fig. 6 shows the surface profiles and average surface roughness S_a given by COM at different immersion times in hydrochloric acid. Corrosion is clearly seen by the topographic images and increasing deviations in the surface profile as well as increased roughness values when the crystals dissolve in the solution. Thus, topographic analysis offered a rapid method to detect also the very early signs of corrosion.

ICP-AES analysis of the hydrochloric acid solution after the immersion of glazes 13 (pseudowollastonite) and 11 (dendritic wollastonite) for different periods of time in hydrochloric acid indicated clearly increased concentrations of calcium and silicon ions (Fig. 7). The calcium ion concentration increased at a faster rate than the silicon ion concentration for both glazes, thus suggesting an incongruent dissolution of the crystals. In addition, minor concentrations of sodium, potassium, aluminum, and magnesium were measured (Table 4). The relative molar ratios of these ions in the solutions corresponded to their ratio in the glassy phase, thus suggesting a slight corrosion of the glassy phase, too. Microscopic analysis after corrosion showed that mainly crystals had corroded while the glassy phase was intact.

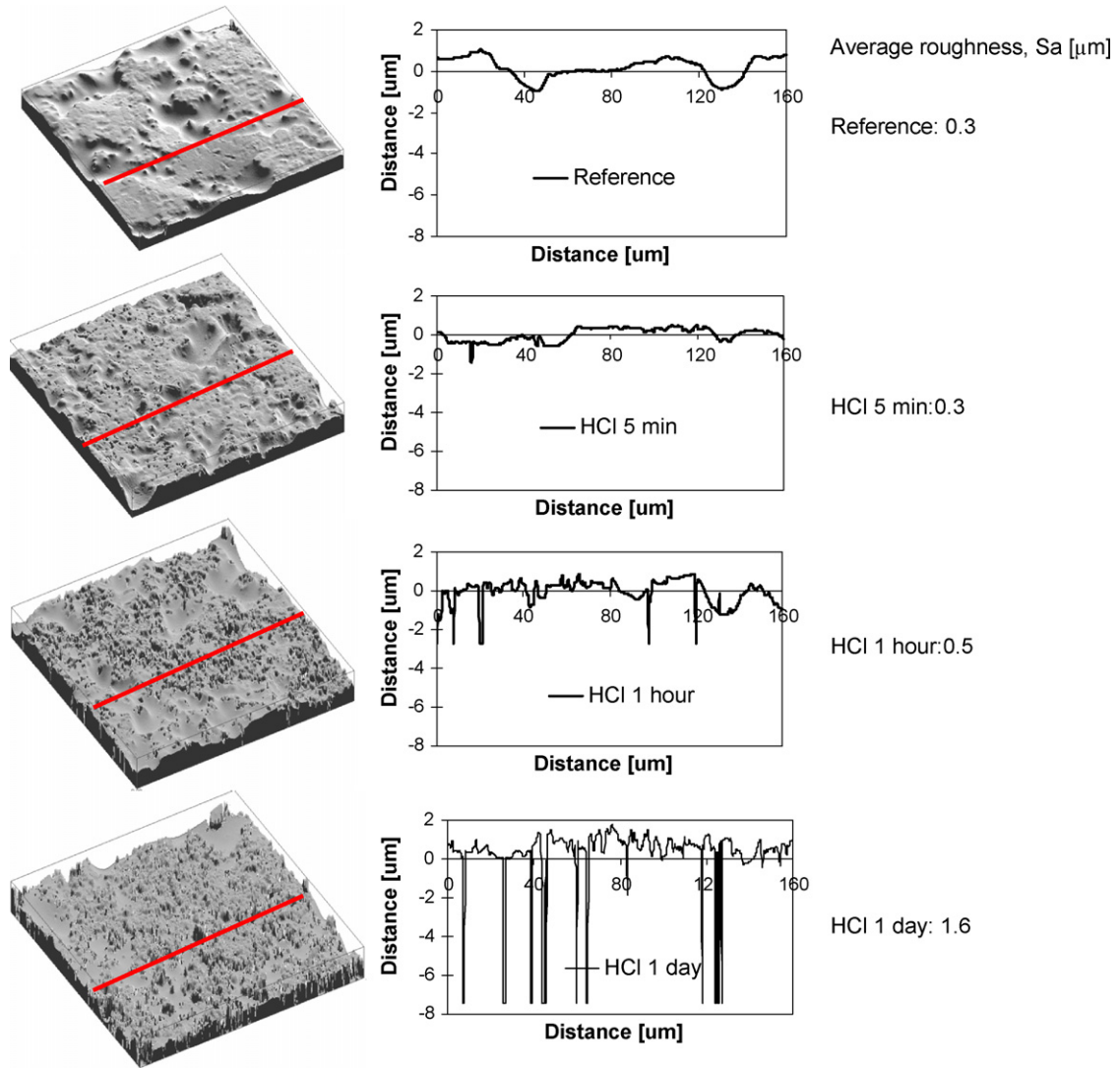


Fig. 6. Topographic image, surface profile and average surface roughness S_a derived from COM analyses for glaze 13 (pseudowollastonite) at different periods of times in hydrochloric acid. Image size: $160 \mu\text{m} \times 158 \mu\text{m}$.

In situ pH measurements of glaze 13 (pseudowollastonite) and glaze 11 (dendritic wollastonite) in hydrochloric acid showed increased values for glaze 13 as a function of immersion time (Fig. 8). The ICP analysis of the solution indicated

much higher calcium than silicon ion concentrations, and only low concentrations of alkali and magnesium ions (Table 4 and Fig. 7). Thus, the pH increase was assumed to be mainly due to an ion exchange reaction of calcium in the crystals with hydrogen ions in the solution.

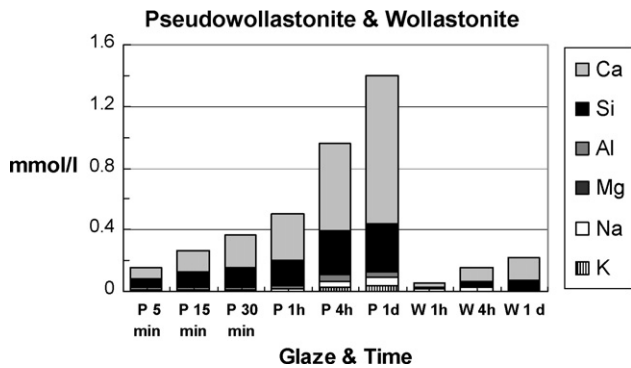


Fig. 7. ICP-AES analysis of the ions dissolved from glazes 13 (P, pseudowollastonite) and 11 (W, dendritic wollastonite) in HCl at different immersion times.

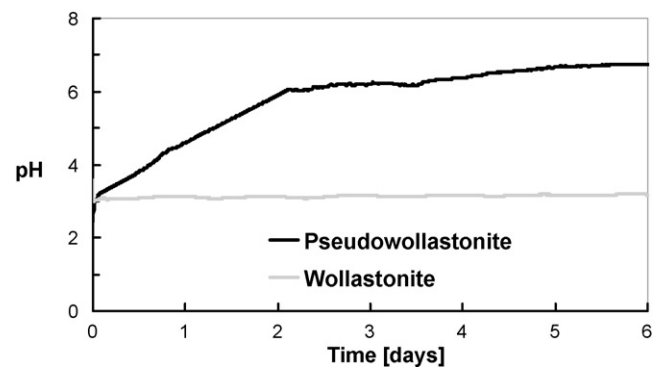


Fig. 8. pH of hydrochloric acid solution at immersion of glazes 13 (pseudowollastonite) and 11 (dendritic wollastonite) for 6 days.

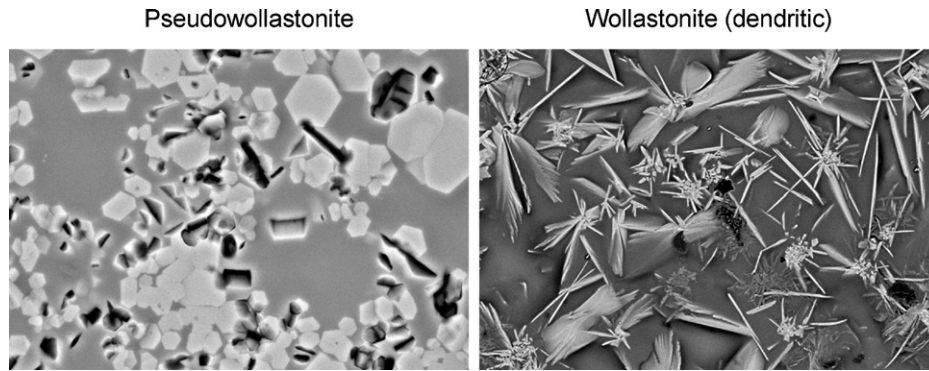


Fig. 9. SEM-micrographs of glazes 13 (pseudowollastonite, attacked) and 11 (dendritic wollastonite, no attack) after 6 days in ultra pure water. The bar equals to 20 μm .

When the glazes were immersed in ultra pure water, a minor increase in pH from roughly 7 to 7.5 was observed for glaze 13 (pseudowollastonite), while no changes in pH were detected for glaze 11 (dendritic wollastonite). SEM-micrographs of the pseudowollastonite glaze after 6 days in water (Fig. 9) showed that some crystals had dissolved. No signs of attack on the wollastonite glaze could be seen in the SEM-micrographs (Fig. 9).

4. Conclusions

The chemical resistance of matte glazes in water solutions clearly depended on the crystal type in the surface. Glazes with diopside showed a good chemical resistance in all test solutions. Glazes with plagioclase crystals were attacked only in very acidic solutions leading to corrosion mainly along the interfacial layers between the crystal and the glassy phase. Wollastonite-type crystals in the surfaces showed poor chemical resistance, and were attacked in acidic to slightly alkaline aqueous solutions. The tiny columnar wollastonite crystals in fast-fired surfaces and hexagonal pseudowollastonite in both fast-fired and conventionally fired surfaces reacted easily in all but the most alkaline test solutions. ICP-AES analysis indicated a faster leaching rate for calcium than silicon, i.e. an incongruent dissolution of these crystals. Formation of pseudowollastonite was avoided in magnesia-containing glazes. The wollastonite crystals in conventionally fired glazes exhibited considerably better chemical resistance. These larger dendritic wollastonite crystals contained some alumina, which was assumed to contribute to their resistance. The results can be applied to adjust the composition of matted glazes for each firing cycle in order to possess surfaces with good chemical resistance in aqueous solutions.

Acknowledgements

This work is part of the Activities of the Åbo Akademi Process Chemistry Centre funded by the Academy of Finland in their Centres of Excellence Program. Funding has been provided by the Clean Surfaces 2002–2006 Technology Programme run by the Finnish Funding Agency for Technology and Innovation (Tekes) and the Graduate School of Materials Research.

References

1. Eppler, R. A., Corrosion of glazes and enamels. In *Corrosion of Glass, Ceramics and Ceramic Superconductors*, ed. D. E. Clark and B. K. Zaitos. Noyes Publications, Park Ridge, NJ, 1992, ISBN 0-8155-1283-X.
2. Kingery, W.D., Bowen, H. K. and Uhlmann, D. R., *Introduction to Ceramics*. John Wiley & Sons, 1976, ISBN 0-471-47860-1.
3. Toya, T., Tamura, Y., Kameshima, Y. and Okada, K., Preparation and properties of CaO–MgO–Al₂O₃–SiO₂ glass–ceramics from kaolin clay refining waste (kira) and dolomite. *Ceram. Int.*, 2004, **30**, 983–989.
4. Toya, T., Nakamura, A., Kameshima, Y., Nakajima, A. and Okada, K., Glass–ceramics prepared from sludge generated by a water purification plant. *Ceram. Int.*, 2007, **33**, 573–577.
5. Cheng, T. W., Effect of additional materials on the properties of glass–ceramic produced from incinerator fly ashes. *Chemosphere*, 2004, **56**, 127–131.
6. Kronberg, T., Hupa, L. and Fröberg, K., Durability of mat glazes in hydrochloric acid solution. *Key Eng. Mater.*, 2004, **264–268**, 1565–1568.
7. Vane-Tempest, S., Kronberg, T., Fröberg, L. and Hupa, L., Chemical resistance of fast-fired raw glazes in solutions containing cleaning agents, acids or bases. In *Proceedings of the VIII World Congress on Ceramic Tile Quality, 1, Qualicer*, 2004, P.GI-155.
8. Hupa, L., Bergman, R., Fröberg, L., Vane-Tempest, S., Hupa, M., Kronberg, T., Pesonen-Leinonen, E. and Sjöberg, A.-M., Chemical resistance and cleanability of glazed surfaces. *Surf. Sci.*, 2005, **584**, 113–118.
9. Bolelli, G., Cannilo, V., Lusvardi, L., Manfredini, T., Siligardi, C., Bartuli, C., Loreto, A. and Valente, T., Plasma-sprayed glass–ceramic coatings on ceramic tiles: microstructure, chemical resistance and mechanical properties. *J. Eur. Ceram. Soc.*, 2005, **25**, 1835–1853.
10. Abdel-Hameed, S. A. M. and El-Kheshen, A. A., Thermal and chemical properties of diopside–wollastonite glass–ceramics in the SiO₂–CaO–MgO system from raw materials. *Ceram. Int.*, 2003, **29**, 265–269.
11. White, W. B., Theory of corrosion of glass and ceramics. *Corrosion of Glass, Ceramics and Ceramic Superconductors*. Noyes Publications, Park Ridge, NJ, 1992, ISBN 0-8155-1283-X.
12. Piispanen, M., Fröberg, L., Kronberg, T., Areva, S. and Hupa, L., Corrosion of glazes coated with functional films in detergent solutions. *Adv. Sci. Tech. (AST)*, 2006, **45**, 156–161.
13. Fröberg, L., Kronberg, T., Törnblom, S. and Hupa, L., Chemical durability of glazed surfaces. *J. Eur. Ceram. Soc.*, 2007, **27**, 1811–1816.
14. Fröberg, L., Vane-Tempest, S. and Hupa, L., Surface composition and topography of fast-fired raw glazes. In *Proceedings of the VIII World Congress on Ceramic Tile Quality, 1, Qualicer*, 2004, P.GI-143.
15. Fröberg, L., Kronberg, T., Hupa, L. and Hupa, M., Influence of firing parameters on phase composition of raw glazes. *J. Eur. Ceram. Soc.*, 2007, **27**, 1671–1675.